

Article

Comparative Genomic Analysis of Phytopathogenic *Xanthomonas* Species Suggests High Level of Genome Plasticity Related to Virulence and Host Adaptation

Juan Carlos Ariute ^{1,2}, Diego Lucas Neres Rodrigues ³, Siomar de Castro Soares ⁴, Vasco Azevedo ³, Ana Maria Benko-Iseppon ^{1,*,†} and Flávia Figueira Aburjaile ^{2,*,†}

¹ Genetics Department, Universidade Federal de Pernambuco, Recife 50740-600, Brazil

² Preventive Veterinary Medicine Department, Veterinary School, Universidade Federal de Minas Gerais, Belo Horizonte 31270-901, Brazil

³ Genetics, Ecology and Evolution Department, Universidade Federal de Minas Gerais, Belo Horizonte 31270-901, Brazil

⁴ Institute of Biological and Natural Sciences, Universidade Federal do Triângulo Mineiro, Uberaba 38025-180, Brazil

* Correspondence: ana.iseppon@ufpe.br (A.M.B.-I.); faburjaile@ufmg.br (F.F.A.)

† These authors contributed equally to this work.

Abstract: *Xanthomonas* bacteria are known phytopathogens difficult to control in the field, which cause great losses in many economically important crops. Genomic islands are fragments acquired by horizontal transference that are important for evolution and adaptation to diverse ecological niches. Virulence and pathogenicity islands (PAIs) enhance molecular mechanisms related to host adaptation. In this work, we have analyzed 81 genomes belonging to *X. campestris*, and a complex group of *X. citri*, *X. axonopodis*, and *X. fuscans* belonging to nine different pathovars and three subspecies, to analyze and compare their genomic contents. *Xanthomonas* pan-genome is open and has a massive accessory genome. Each genome showed between three and 15 exclusive PAIs, well conserved through strains of the same pathovar or subspecies. *X. axonopodis* pv. *anacardii* had higher general similarity to *X. citri* subsp. *citri* and *X. fuscans* subsp. *aurantifolii*, with which a few PAIs were shared. Genomic synteny was even for almost all strains, with few rearrangements found in *X. axonopodis* pv. *anacardii*. The prophage regions identified in the genomes were mostly questionable or incomplete, and PAI13 in *X. campestris* pv. *campestris* ATCC33913 matched a prophage region of 19 transposable elements. Finally, PAIs in *Xanthomonas* are pathovar-specific, requiring individual strategies of combat.

Keywords: genomic islands; host adaptation; pangenomics; pathogenicity; phytopathology



Citation: Ariute, J.C.; Rodrigues, D.L.N.; de Castro Soares, S.; Azevedo, V.; Benko-Iseppon, A.M.; Aburjaile, F.F. Comparative Genomic Analysis of Phytopathogenic *Xanthomonas* Species Suggests High Level of Genome Plasticity Related to Virulence and Host Adaptation. *Bacteria* **2022**, *1*, 218–241. <https://doi.org/10.3390/bacteria1040017>

Academic Editor: Bart C. Weimer

Received: 19 July 2022

Accepted: 27 September 2022

Published: 8 October 2022

Publisher's Note: MDPI stays neutral with regard to jurisdictional claims in published maps and institutional affiliations.



Copyright: © 2022 by the authors. Licensee MDPI, Basel, Switzerland. This article is an open access article distributed under the terms and conditions of the Creative Commons Attribution (CC BY) license (<https://creativecommons.org/licenses/by/4.0/>).

1. Introduction

Bacteria of the genus *Xanthomonas* affect several crops of economic importance, responsible for diseases such as bacterial black spot, citrus canker, and the bacterial canker of grapevine, for instance [1,2]. Even though these phytophobioses cause considerable economic losses [3], there is still no adequate method to control their spread and reduce disease incidence in agriculture, specially those associated with *X. campestris* and *X. citri* [4–7]. Studies regarding this and other *Xanthomonas* species, revealed the enormous potential of comparative genomics approaches focused on the accessory genome and mobile elements to elucidate aspects of pathogenicity explicitly assigned to adaptive traits, cell physiology, and host specificity [8–12]. When applied to different pathovars of the same species, this type of approach aids in plant-host relationship studies, since it is possible to identify specific genes and metabolic pathways based on the genome structure and composition as well [13]. Consequently, studies for the identification and characterization of virulence factors and protein effectors shared with different strains of the same species allow the

discovery of specific genomic profiles suggesting an increased or reduced virulence for a given host [14–16].

Previous studies based on the morphology and other phenotypic characteristics of *Xanthomonas* have misclassified it taxonomically, such as strains that infect grape, cashew, and mango crops, amongst others [17]. As whole genome-based techniques were improved, topologies in the *Xanthomonas* genus were changed in many species. For instance, whole-genome sequencing, DNA–DNA hybridization and multilocus analyses in strains of *X. axonopodis* have shown biased taxonomy in species, subspecies, and pathovar levels, supporting reclassification to *X. citri* pv. *anacardii* *X. citri* pv. *vignicola*, and *X. citri* pv. *glycines* instead [18]. Moreover, other phylogenies confirmed with these new topologies, reclassifying *X. fuscans* as a pathovar of *X. citri*, and *X. albilineans* would form a joint clade linking the *Xanthomonas* genus to *Xyllela fastidiosa* [19]. Similarly, recent phylogenetic and ANI (average nucleotide identity) analyses have supported transference of *X. campestris* pv. *arecae* and *X. campestris* pv. *musacearum* strains to *X. vasicola* [20].

Even though those species might be similar, it has not yet been elucidated how similar their genomic features as a whole might be, including the dispersion of molecular features related to pathogenicity. Thereby, this study aims to understand the influence of the genomic content of the *X. citri* complex and *X. campestris* on virulence, pathogenicity, and the specific host–pathogen correlation.

2. Materials and Methods

2.1. Genome Annotation of *Xanthomonas* species

We obtained 80 complete genomes from the National Centre for Biotechnology Information (NCBI) belonging to *X. citri* and *X. campestris* species. The genomes of those species were selected due to the interest of the research group in species that affect agriculture in Northeast Brazil. All genomes are listed in Table A1, according to their strain, isolation source, and related disease.

2.2. Genomic Characterization and Enrichment Analysis

Initially, all genomes were automatically annotated by Rapid Annotation using Subsystem Technology (RAST) performed to predict putative CDSs, tRNA, and rRNA regions [21]. Subsequently, we used the Artemis tool [22] for manual gene characterization according to alignments done at UniProt, Pfam, and InterProScan databases. To carry out genetic enrichment, we used the Gene Ontology Functional Enrichment Annotation Tool (GO Feat) [23] for the characterization of genes and proteins at three different ontological levels (molecular function, biological process, cellular component) of all 80 genomes of *Xanthomonas* strains. We also used the Kyoto Encyclopedia of Genes and Genomes (KEGG) [24] to characterize metabolic pathways for both pangenomes and individual sets of genomes. We only performed the characterization for individual sets of genomes to *X. citri* and *X. campestris*, due to the low number of representative *X. vasicola* genomes available.

2.3. Pan-Genome Analyses

For the pan-genome analyses, we used Bacterial Pan-Genome Analyses pipeline (BPGA) [25] to identify clusters of orthologous sequences (COG) among *Xanthomonas* genomes. We also used Roary [26] for phylogenomic inference and FigTree [27] for phylogenomic tree visualization. Finally, we used the Virulence Factor Database (VFDB) [28] to determine a cluster map of virulence factors throughout all *Xanthomonas* genomes.

2.4. Prediction and Characterization of Pathogenicity Islands

We used the Genomic Island Prediction Software (GIPSy) tool [29], which is one of the most cited and recommended tools in the literature [30], to obtain genomic islands in all genomes, focusing on pathogenicity islands (PAIs). Then, we added and correlated GO terms to CDS in each pathogenicity island in *X. citri* and *X. campestris* strains. In this step, we only considered exclusive PAIs, since many regions were associated with more than

one type of genomic island (metabolic, resistance, or symbiotic). We used BLAST Ring Image Generation (BRIG) [31] to represent and evaluate the position of genomic islands in different strains of *Xanthomonas*, as well as the similarity between strains of the same and different pathovars and/or subspecies. To understand island distribution and conservation through different genomes, the graphs were plotted using representative pathovars, each with a reference strain, so that the relationships between PAIs and hosts would be easier to approach. We chose genomes with the highest number of PAIs as representative genomes for each pathovar. The faded regions in the rings denoted lower similarity (<70%) whilst strong colors denoted higher similarity (>90%). We also used the MAUVE tool [32] to identify probable genomic rearrangements among strains of interest by comparing strain-specific regions correlated with genomic islands of reference strains and checking if there were any disruption, change of location, or change of sense between different strains.

2.5. Subcellular Localization of Proteins inside PAIs

The online platform PSORTb v.3 [33] was used to predict the subcellular location of the coding sequences products inside pathogenicity islands of interest. Specific multifasta files were manually created for each island of interest, with sequences available in the Artemis interface.

2.6. Prediction of Prophages Regions in *Xanthomonas* genomes

We performed a comparison of prophage regions between different pathogens using PHASTER [34]. This tool identified and classified each prophage region in representative pathovars of *X. citri* and *X. campestris* according to scoring in three categories: intact (score green > 90), questionable (score blue 70–90), and incomplete (score red < 70).

3. Results

3.1. Functional Genomics and Comparative Genomics Insights of *Xanthomonas* species

All 80 genomes presented around 65% GC content, all relevant information regarding strains is available in Table A1. The automatic annotation on RAST predicted 4287 coding sequences (CDS) in the selected reference genome *X. campestris* pv. *campestris* ATCC 33913. The GO results for all 80 strains' genomes showed that most proteins are involved in molecular functions, representing a percentage higher than 1/3 of the total protein repertoire. The other two categories, biological processes and cellular components ranged from 1925 to 2223 and 1509 to 1813 proteins, respectively (Figure S1). Overall, the COG profile of both *X. campestris* and *X. citri* were very similar. Categories of general or unknown function (R and S) had the highest percentages (around 40% and 20%, respectively) in the core, accessory, and unique genomes of these two species, possibly due to the lack of studies on the functional characterization of representative genomes. Other categories of COG with considerable percentages of genes were related to (1) cell wall/membrane/envelope and biogenesis, (2) signal transduction mechanisms, (3) intracellular trafficking, secretion, and vesicular transport, and (4) transcription (Figure S2). For the pan-genome analysis, the distribution of unique, accessory, and core genomes among the categories was almost uniform, except for nucleotide transport and metabolism, in which no unique genes were identified for *X. citri*, and a small portion of unique with no accessory genes found for *X. campestris* (Figure S2). Roary prediction of genome shows that the accessory genome of *Xanthomonas* had a higher number of genes compared to the core and unique genomes, corroborating with BPGA analysis (Figure S3) (Table 1). Moreover, BPGA results indicate the pan-genome is still open, as the alpha value was lower than 1. However, as the curve flattened and stabilized with the increasing number of genomes added to the analysis, it may be closed soon enough, as seen in Figure 1.

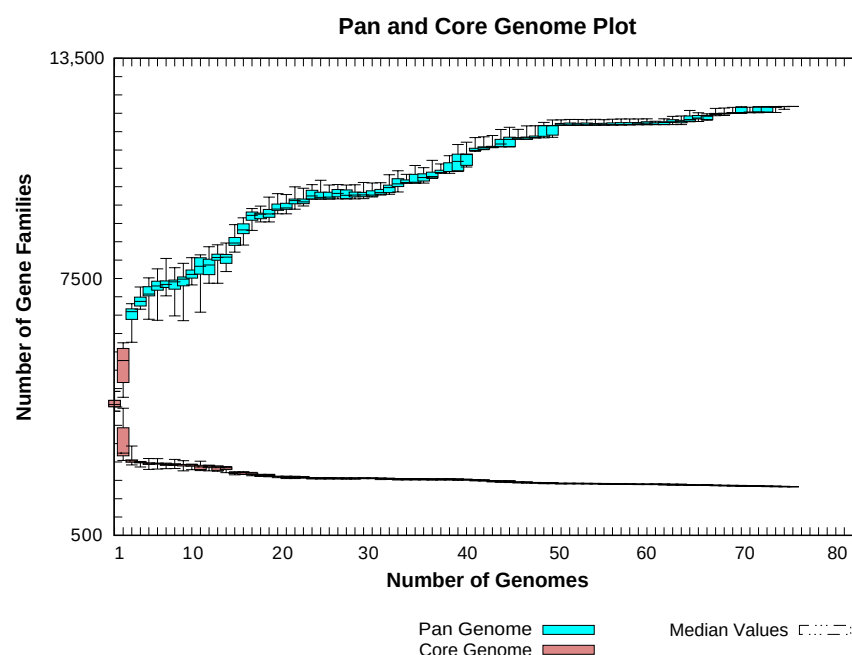


Figure 1. Curve of *Xanthomonas* genus pan-genome development calculated with all 80 genomes.

Table 1. Pan-genomes results (core, accessory, and unique) for *X. campestris* and *X. citri* genomes individually, and *Xanthomonas* genus pan-genome with all 80 genomes.

	Core	Accessory	Unique
<i>Xanthomonas</i>	2585	2750	11,562
<i>X. campestris</i>	3413	1813	1173
<i>X. citri</i>	2936	2561	9055

Agreeing to that, the distribution of metabolic pathways on KEGG for the *Xanthomonas* pan-genome showed that some categories had more sequences belonging to the accessory genome than to the core, specifically categories that are somehow related to pathogenicity and virulence, such as cell motility, glycan biosynthesis and metabolism, infectious diseases, membrane transport, signal transduction, xenobiotics degradation and metabolism (Figure 2). General categories like cellular processes and environmental information processing also showed more genes related to the accessory pan-genome. The pan-genome matrix based on the core genome revealed that *X. campestris* exhibited clusters of genes different from the other species' genomes (Figure S4). The core phylogenomic tree on this figure is also available in Figure S5.

Finally, the search for virulence factors revealed 14 genes present through the genomes, but only 4 were identified in all 81 genomes: *htpB*, *pilG*, *cheY*, and *fliN*. Other virulence factors such as *pilT*, *vipB*, *clpV1*, *ugd*, and *vipA* were also common for most of the genomes. Only the genomes of *X. campestris* pv. *raphani* 756C, *X. citri* subsp. *malvacearum* XcmN1005 and *X. citri* subsp. *malvacearum* MS14003 presented exclusive virulence factors *fliA* and *pilC*, respectively. A cluster map for all virulence factors is available in Figure S6.

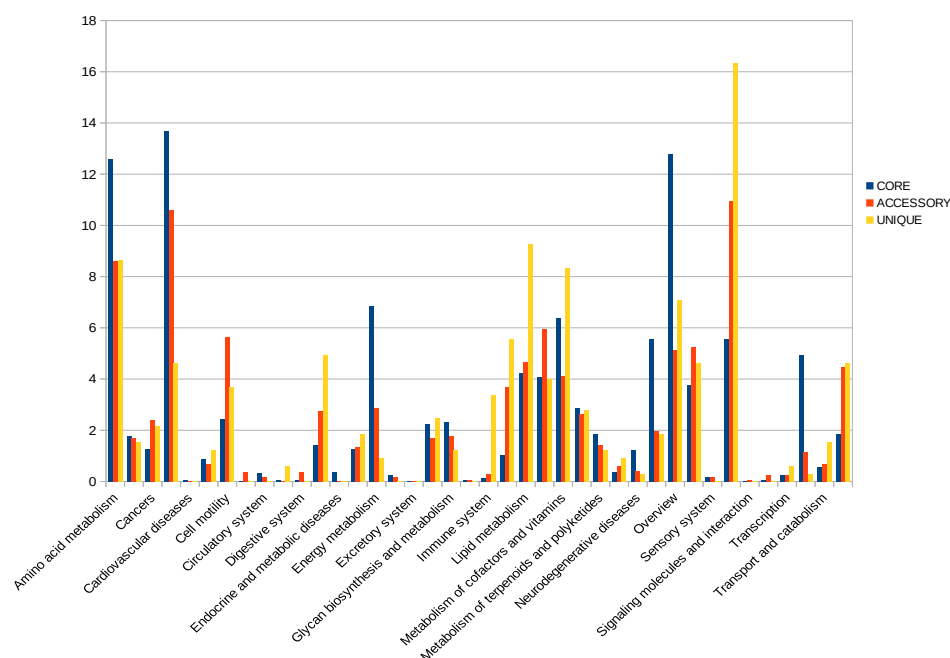


Figure 2. KEGG metabolic pathways on the total pan-genome of *Xanthomonas*.

3.2. Genomic Islands Reveal a New Potential Regarding the Pathogenicity of the Genus

All genomes analyzed presented PAIs, and most of them matched with genomic regions of GC content deviation. The genomes of *X. campestris* pv. *campestris* 17, *X. citri* pv. *fuscans* ISO118C5, *X. citri* pv. *fuscans* ISO118C3, *X. citri* pv. *phaseoli* var. *fuscans* CFBP6167 and *X. citri* pv. *phaseoli* var. *fuscans* CFBP6996R presented only three PAIs, making the lowest number found in this analysis. On the other hand, *X. citri* subsp. *malvacearum* XcmH1005 exhibited the highest quantity, with 15 exclusive PAIs. The total number of PAIs found for all genomes is available in Table A2. Most of the islands found on the genomes constituted CDSs annotated as hypothetical proteins, only being able to infer their function based on the enrichment analysis. Among the *X. citri* subsp. *citri* genomes, strain TX160197 exhibited the highest number of PAIs (14) and high genomic similarity with other strains, except for AW13, AW14, AW15, AW16, TX160042, and TX160149. Besides, all different strains from this subspecies exhibited similarity below 70% for PAI24 and gaps inside this genomic region (Figure 3). As for *X. campestris*, strain ATCC 33913 contained ten PAIs, of which most were highly conserved in this species' strains, except for strain 17 and *X. campestris* pv. *raphani* 756C. As for *X. vasicola* pv. *arecae* NCPB2649 and *X. vasicola* pv. *musacearum* (Figure 4).

The previous scenario was similar for *X. citri* subsp. *malvacearum*: PAIs in the reference strain XcmH1005 had high conservation, although gap regions were present in large islands, such as PAI14 (Figure 5). However, in *X. citri* pv. *phaseoli* var. *fuscans*, almost all islands found in the selected reference strain CFBP7767 consisted of gap regions in the other strains of this pathovar, except for strains CFBP6992 and CFBP4885 (Figure 6), also similar to what was observed in genomes of *X. citri* pv. *fuscans*.

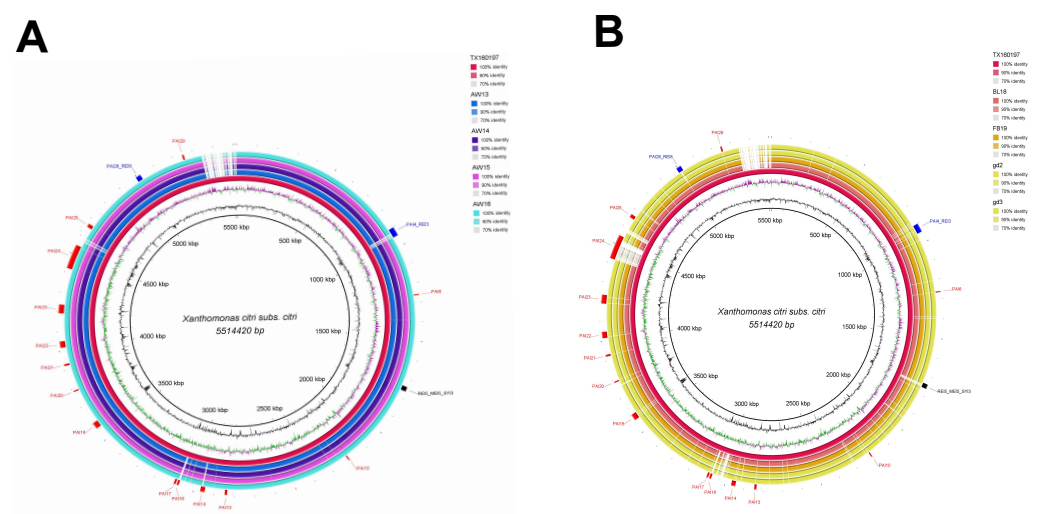


Figure 3. Alignments of *X. citri* subsp. *citri* genomes and their genomic islands. PAI24 is well conserved for (A) strains AW13, AW14, AW15, and AW16, but not for others such as (B) BL18, FB19, gd2, and gd3. It is possible to observe that PAI24 does not present the complete region in the strains BL18, FB19, gd2, and gd3 showing a low identity (<70%) region.

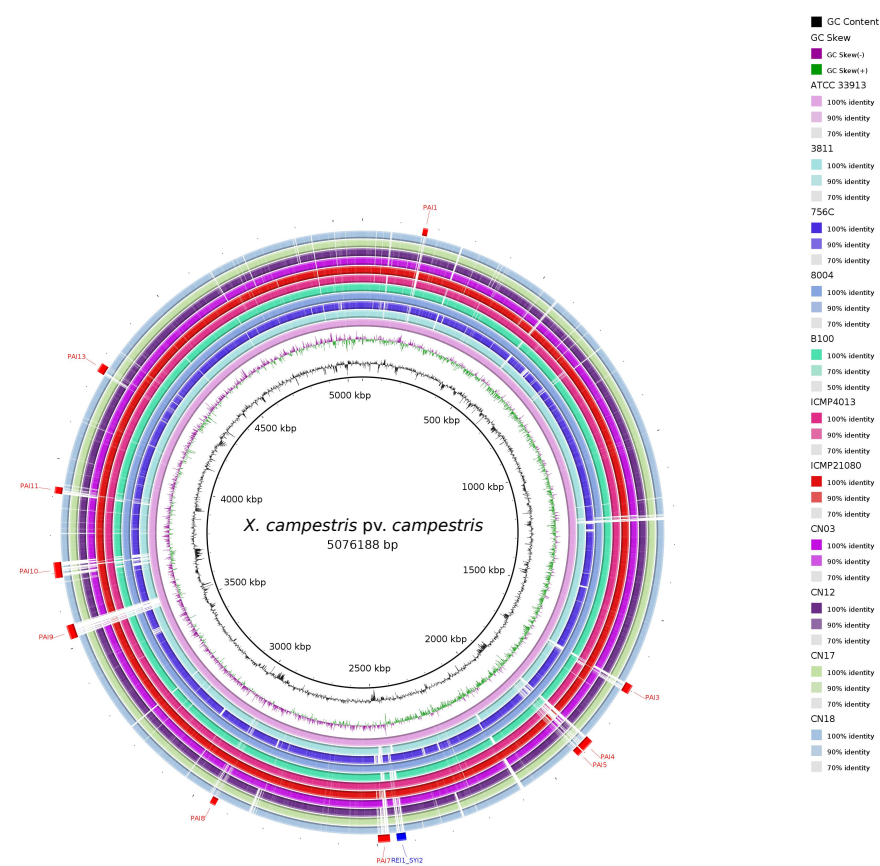


Figure 4. Alignments of *X. campestris* genomes and their genomic islands.

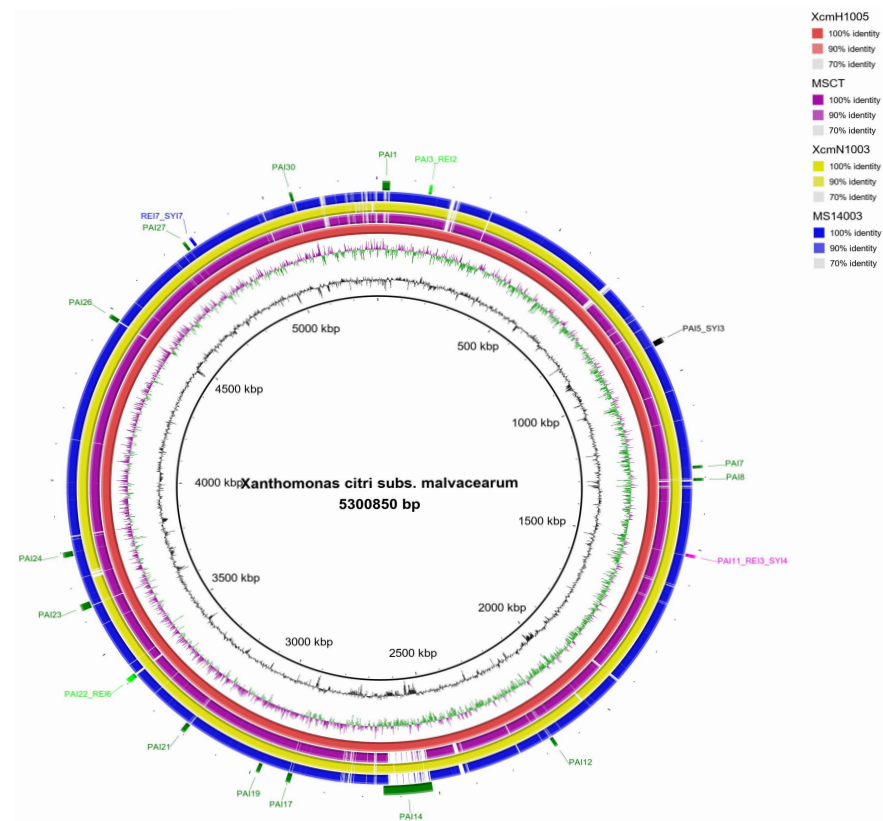


Figure 5. Alignments of *X. citri* subsp. *malvacearum* genomes and their genomic islands. Strain XcmN1003 (yellow ring) presents the highest similarity amongst other strains of the same pathovar.

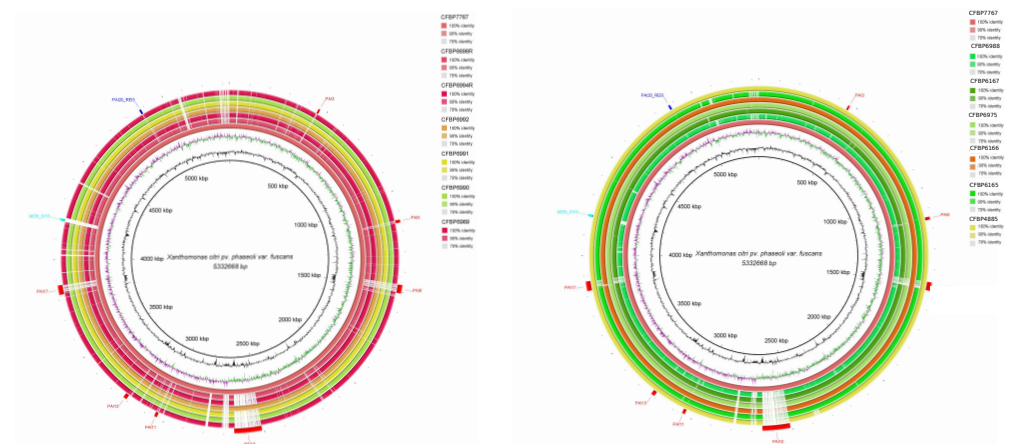


Figure 6. Alignments of *X. citri* pv. *phaseoli* var. *fuscans* genomes and genomic islands. The strain CFBP 7767 (inner-central ring) has the highest similarity among other strains of the same pathovar.

For *X. citri* pv. *aurantifolii* genomes, strain FDC1559 presented 11 well-conserved and exclusive PAIs. Moreover, strain 1566 had a similarity of 100% with the reference genome (Figure 7). For *X. citri* pv. *vignicola*, *X. citri* pv. *anacardii*, *X. axonopodis* pv. *vignicola*, and *X. axonopodis* pv. *anacardii*, most of the PAIs identified in the reference genome were gap regions in the other strains (Figure 8). Finally, *X. citri* pv. *glycines* exhibited the highest conservation of pathogenicity islands among their strains (Figure 9).

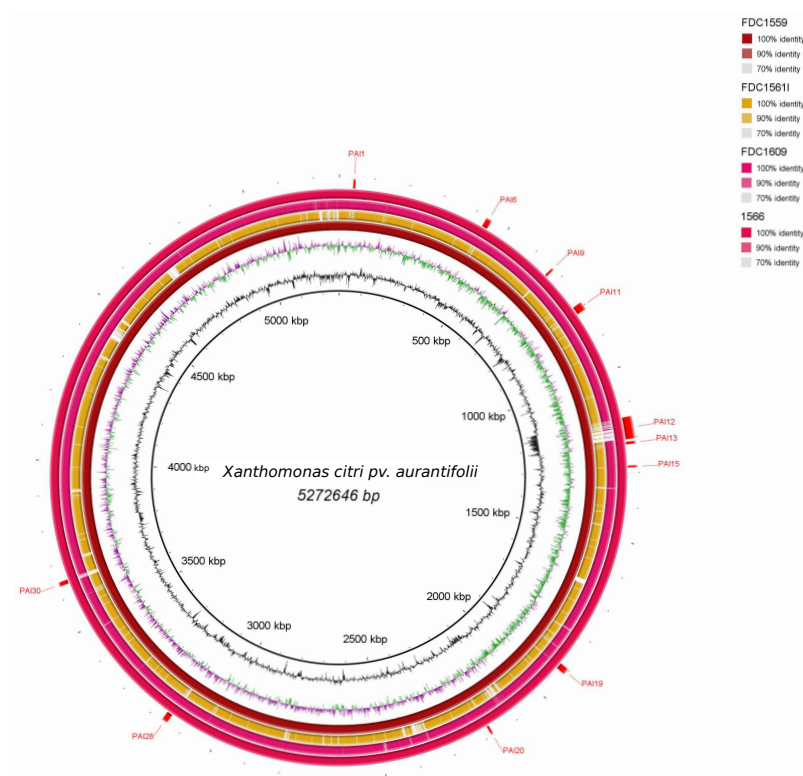


Figure 7. Alignments of *X. citri* pv. *aurantifolii* genomes and genomic islands. Strain FDC1559 (brown inner ring) has the highest similarity among other strains of the same pathovar in this species.

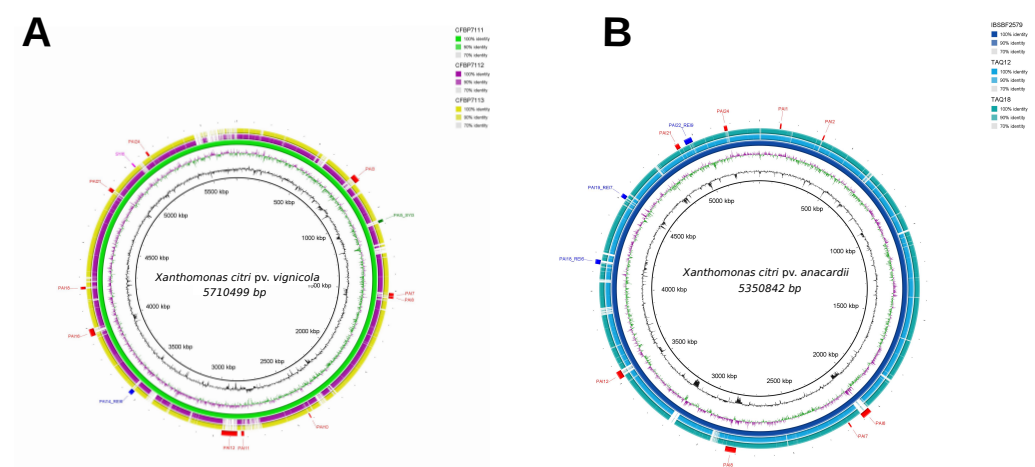


Figure 8. Alignments of *X. citri* pv. *vignicola* (A) and *X. citri* pv. *anacardii* (B) genomes and their genomic islands. Almost all pathogenicity islands identified in reference strains CFBP7111 (A), and IBSBF2579 (B) consisted of gap regions in the other strains.

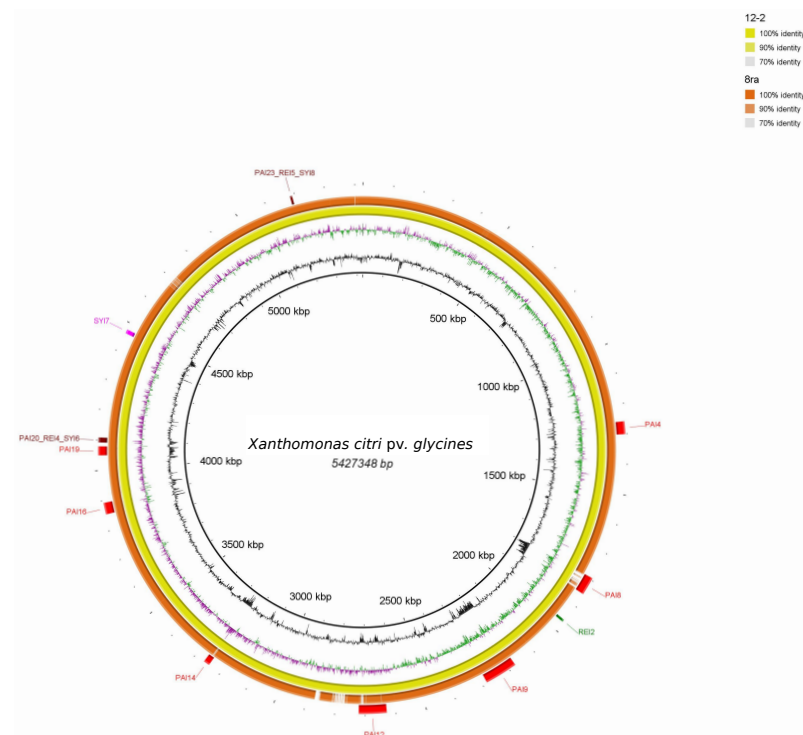


Figure 9. Alignments of *X. citri* pv. *glycines* genomes and genomic islands. All pathogenicity islands identified in reference strain 12-2 are conserved in strain 8ra, except for PAI5.

As for interspecies comparisons, genomes of *X. axonopodis* pv. *anacardii* showed high genomic identity when compared against the genome of *X. campestris* pv. *campestris* ATCC 33913. However, none of the PAIs identified in the latter showed high conservation amongst *X. axonopodis* pv. *anacardii* genomes, as most of its PAIs, matched with significant genomic gaps (Figure 10). In contrast, PAIs found in *X. citri* subsp. *citri* TX160197 had higher conservation and similarity. Similar profiles were observed for PAIs in *X. citri* subsp. *malvacearum* Xcmh1005, *X. citri* pv. *phaseoli* var. *fuscans* CFBP7767, *X. axonopodis* pv. *vignicola* CFBP7111 and *X. axonopodis* pv. *glycines* 12-2. The highest similarity of PAIs was observed in comparison with the genome of *X. fuscans* subsp. *aurantifolii* FDC1559 (PAIs 6, 11, 12, and 28) (Figure 11).

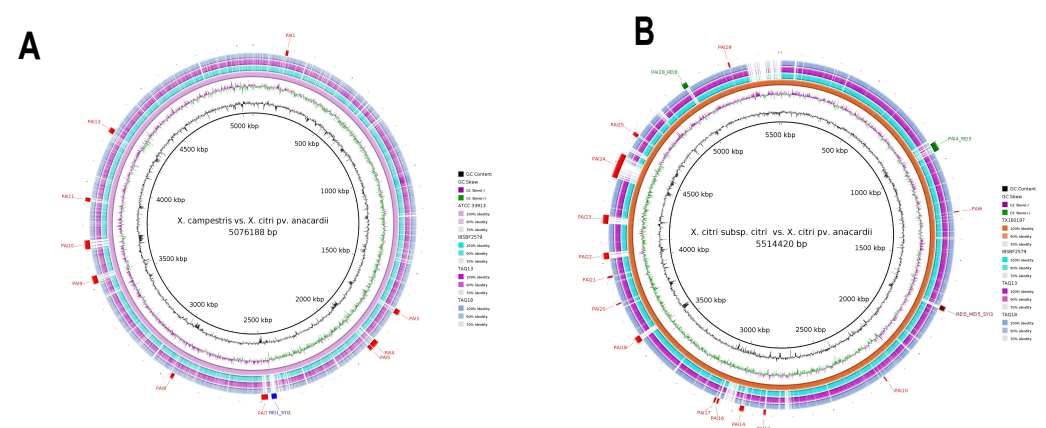


Figure 10. Genomic islands comparisons with (A) *X. campestris* pv. *campestris* ATCC33913 and (B) *X. citri* subsp. *citri* TX160197 against strains of *X. citri* pv. *anacardii*. The islands showed higher similarity for *X. citri* subsp. *citri* genomes than for *X. campestris*, but no genomic islands of both species were conserved in *X. citri* pv. *anacardii* genomes.

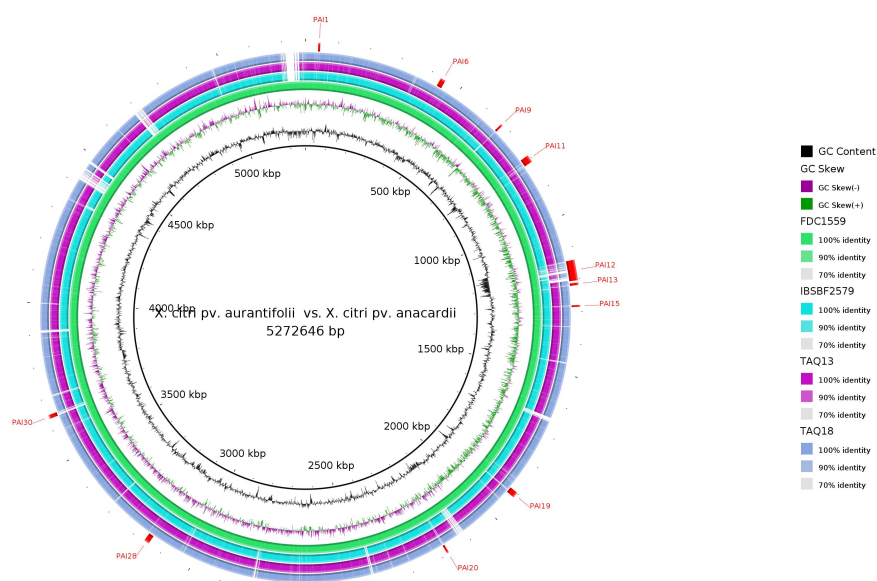


Figure 11. Genomic islands comparisons with *X. citri* pv. *aurantifolii* FDC1559 against strains of *X. citri* pv. *anacardii*. The similarity panel was almost even for both species.

Although some of these islands were conserved in different pathovars, they presented different levels of integrity. An example is CDS XCG122_1740, a virulence regulator located in PAI8 of *X. citri* pv. *glycines* 12-2, which suffered an inversion in *X. citri* pv. *anacardii* IBSBF2579 PAI6, corresponding to CDS IBSBF_1976 (Figure S7). On the other hand, some genomic islands exhibited exceptional conservation in certain strains of the same pathovar, exhibiting almost no changes, such as for PAI21 of *X. citri* pv. *vignicola* CFBP7111, CFBP7112, and CFBP7111 (Figure S8).

3.3. Cellular Localization and Ontology of Pathogenicity Islands

Most PAIs contained hypothetical proteins that were secondly annotated as putative virulence factors, such as sequences related to carbohydrate metabolic process (GO:0005975), hydrolase activity (GO:0016787), DNA-binding transcription factor activity (GO:0003700), and signaling receptor activity (GO:0038023).

Subcellular analysis of 28 well-conserved PAIs indicated that most proteins had cytoplasmic or unknown cellular localization. Only 119 coding sequences had different localizations, while only nine were described as extracellular proteins: three found in *X. citri* pv. *anacardii* IBSBF2579, one in *X. citri* pv. *vignicola* CFBP7111 and *X. citri* pv. *aurantifolii* FDC1559, and two in *X. citri* pv. *glycines* 12-2 and *X. citri* pv. *fuscans* ISO188C1 genomes. No extracellular proteins were found in well-conserved PAIs belonging to *X. campestris* or other *X. citri* genomes. Finally, five proteins were found for the outer membrane, and 15 proteins might be in multiple positions inside the cell. All the other proteins found were for cytoplasmic membrane location.

3.4. Prophage Regions, Transposable Elements and Their Relationship with Pathogenicity Islands

The highest numbers of prophage regions were observed in genomes of *X. citri* pv. *aurantifolii* strain FDC1609 (3 intact, 2 questionable and 7 incomplete), strain 1566 (2 intact, 2 questionable and 3 incomplete) and *X. citri* pv. *vignicola* CFBP7111 (4 intact and 4 incomplete). Regions that corresponded with many incomplete prophages were found in the genomes of *X. campestris* pv. *raphani* 756C (regions 1 and 3), *X. campestris* pv. *campestris* CN15 (regions 2 and 3), B100 (region 2), ICMP 21080 (region 4) and ICMP 4013 (region 12). Two regions of intact phages were detected in the genomes of *X. vasicola* pv. *musacearum* NCPPB 4379 and *X. campestris* pv. *campestris* 8004. The number of prophage regions found for each genome is available in Table A3.

Interestingly, some genomic islands and prophage regions overlapped. For instance, in the genome of *X. campestris* pv. *campestris* ATCC33913, PAI13, a genomic island of identity above 90% when compared against other genomes of the same species, comprehended mostly insertion sequences (IS) transposases and matched a region of an intact prophage. Those sequences belonged to the Isxccc1 and IS3 families (19 out of 23 CDSs), and others were annotated as phage-related proteins. The different sequences were putative virulence factors related to molecular functions, such as carbon-sulfur lyase activity (GO:0016846) and oxidoreductase activity (GO:0016491). In addition, many transposable elements in well-conserved PAIs were seen in PAIs 23 and 24 of *X. citri* subsp. *citri* TX160197, PAI4 of *X. citri* subsp. *malvacearum* AR81009 (which was well conserved in the genomes of strains XcmH1005 and XcmN1003, but not in MSCT and MS14003), and PAIs 11 and 12 of the *X. citri* subsp. *malvacearum* AR81009 PAI11. The genome of *X. citri* pv. *phaseolis* var. *fuscans* CFBP7767 showed sequences related to bacterial conjugation, pili, transposases, and virulence factors within PAI13. As for *X. citri* pv. *anacardii* IBSBF2579 genome, PAI8 was not only counted with many transposable elements but also a few putative virulence factors as well. However, this region did not match any prophage region detected in the genome, intact or not.

4. Discussion

4.1. Insights Provided by the Pan-Genome of *Xanthomonas*

Some pangenomics studies on certain species of *Xanthomonas* have been carried out to find out what makes strains more or less virulent. For instance, pan-genome tools have been addressed to aid in taxonomy revisions of *X. arboricola*, and also to find relationships between different lineages of *Xanthomonas* species based on the core genome [35–37]. Some effectors, such as TALEs and T3SEs, are present in most strains of *X. citri* pv. *glycines*, indicating a closed pan-genome due to low differences in genomic content [38,39]. For *X. perforans*, however, it has been found that most of the pan-genome is made of more than 4000 genes present in accessory genomes, indicating an open genome due to recombination mechanisms of this species [16]. Studies on the sister clade of *Xanthomonas* and *Stenotrophomonas* have shown that almost only 10% of the genes make part of a core genome of this genus [40]. In the present study, we described the pan-genome for the most representative species of the genus. We suggest the reason it is still open is due to a high diversity of accessory genomes, especially regarding their pathogenicity traits. These results open new perspectives for the study of evolutionary genomics of *Xanthomonas*, focusing on their accessory genomes.

4.2. Enrichment Analysis in Pathogenicity Islands

The genomic features annotation was more in-depth than in previous studies [41,42], considering mainly the number of identified pseudogenes. Moreover, the high percentage of unique genes with general or unknown functions in *X. citri* strains had already been associated with its wide range of diversification [43]. Two significant characters of integrative conjugative elements (ICE) are found in a high number of *Xanthomonas* PAIs: integrase-like sequences and type IV secretion systems (T4SS) genes. Since ICEs may also originate from genomic islands, the high quantity of these types of sequence may indicate *Xanthomonas* might have acquired genomic islands through ICE events, and the well-conserved ones among strains are those containing mobile elements encoded by ICE [44]. Furthermore, as PAIs evolve to carry only the genes essential for their maintenance and transference [45], considering the PAIs here identified lack the usual genetic features commonly associated with pathogenicity (such as virulence factors, toxins, adhesins, and others), perhaps the genomic islands of *Xanthomonas* might have already gone through strong evolutionary pressure. As seen in Figure S7, a few putative virulence factors changed their genomic syntenic region when transference occurred, which may indicate genome shuffling. Although component genes of T4SS were not directly associated with virulence in different *Xanthomonas* species, the presence of T4SS genes in PAIs is essential because it may aid in

interspecific competition whenever contact between different plant microbiome bacteria happens, thus, facilitating host colonization [42,46]. Our results present significant ontological terms of biological, molecular, and cellular processes implicated in pathogenicity and bacterial virulence. Considering biological process features analysis, a considerable number of GO terms classified as DNA-mediated transposition was found in genomes of *X. citri*. The recombinant DNA-mediated gene can produce xanthan gum, which is essential for colonization and bacterial growth [47,48], promoting infection success. In molecular mechanisms, genes encoding type III effectors play a crucial role in plant–pathogen interaction, stimulating defense responses [49,50]. Sequences related to the nucleic acid-binding ontology, present in most PAIs, have already been described in *X. campestris* [51]. Those proteins may act as catabolic factors and are involved in phytopathogenesis regulation; however, it is important to note that not only nucleic acid-binding proteins are responsible for gene regulation [52]. Activities related to the growth and proliferation of bacteria within the host are also associated with the presence of iron-sulfur binding proteins, essential for micronutrient acquisition required for pathogenic bacteria [53–55]. They play critical roles in the control of many cellular activities essential to pathogenicity, such as metabolic pathways and intracellular transport molecules [56]. Genomic evolution studies of *X. campestris* pv. *campestris* and *X. citri* pv. *citri* identified 30 genomic islands that originated from the lateral transference of genes [57]. This suggests that it could be associated with the improved ability of a pathogen to adapt to specific environments and/or hosts. In our study, homologous genes for resistance were found on the pathogenicity islands as well. Metallopeptidases, for instance, are typically associated with catalytic activities such as the cleavage of reactive oxygen species (ROS) in dismutation reactions [58]. The burst of ROS has an antimicrobial effect on the plant cell, so those genes are associated with defense within the host [59]. It demonstrates how genes located in PAIs do not strictly act as virulence factors but may also aid in the pathogen protection against natural defenses on host.

Finally, this work is the first study to carry out an in-depth comparative analysis of *Xanthomonas* species presenting ontological characterization and excellent curation of genes and their predicted products in these complete genomes. The pathogenicity island analysis revealed an essential role in the infection process and a wide field for experimental investigation in pathways acting directly on plant–pathogen response. Due to the environmental microbial diversity, this community undergoes selective pressures over the years, making it difficult to understand the association of a pathovar/disease to a particular genomic repertoire. More studies aimed at the microbial community can open a potential spectrum on this subject. Due to the high similarity among PAIs belonging to *X. citri* pv. *anacardii*, *X. citri* pv. *glycines* and *X. citri* pv. *fusca* strains, we propose that those pathovars might have similar virulence mechanisms. Therefore, the same methods for diagnostic and preventive treatment might also be considered for the affected crops. The response mechanism that those different hosts display to stop these pathogens also needs to be considered.

4.3. Prophage Regions and the Evolution of Bacterial Phytopathogens

Many studies have tried to infer the origin and role of prophage regions in bacteria to elucidate a disease or the ability to interact with the host; nevertheless, the mechanisms still seem unknown [60,61]. Plant–pathogen interactions allow a high genetic variation and exchange both between the environment and between the host, so the higher is the host range of a pathogen, the higher genetic variability it displays. Transposable element insertion may alter the frame of determining genes, reducing or increasing their expression level and, therefore, affecting bacterial virulence. The presence of many genetic elements in these genomes reinforces the occurrence of past recombination or horizontal transfer events [8].

Prophage regions have already been reported for *X. campestris* pv. *campestris* ATCC 33913, attributed to insertion events before the evolution and separation events among *X. campestris* and *Xanthomonas oryzae* species, with identity superior to 90% [60]. Since we observed overlapping regions with PAIs and prophage sequences, it suggests that phage insertions occurred in one original strain and disseminated through genomic island sharing events. Most strains of the same pathovar were obtained in the same geographical region, reinforcing that they probably shared those genomic regions before the diversification of those species.

5. Conclusions

Overall, the participation of pathogenicity islands in the *Xanthomonas* genus' accessory genome is undeniable since most islands were specific in each lineage subgroup, despite the overall great genomic similarity. Up until now, a significant part of *Xanthomonas*' molecular features is still unknown, and as they are also present in PAIs, they may contain vital information for understanding its virulence. On this thought, future studies are fundamental to help understand pathogen-host relationships better, and that knowledge would also influence the development of preventive biotechnological tools in modern agriculture, especially for plant immunization. A broad accessory pan-genome influencing pathogenicity means developing specific strategies to fight each pathovar on their own, but a soon-to-be-closed pan-genome means those strategies might be effective for a considerable time. In addition to that, the characterization of the different PAIs investigated in this study suggests that some may be indirectly involved in virulence, as many of them contain transposable elements that can alter the actual genomic configuration and control of gene expression originating from past phages. Finally, *Xanthomonas* bacteria are highly adapted to phytopathogenicity due to their big genetic arsenal.

Supplementary Materials: The following supporting information can be downloaded at: <https://www.mdpi.com/article/10.3390/bacteria1040017/s1>.

Author Contributions: Conceptualization, supervision, writing—review and editing: F.F.A. and A.M.B.-I.; methodology, formal analysis, and data curation: J.C.A. and D.L.N.R.; writing—original draft preparation: J.C.A.; writing—review and editing: S.d.C.S. and V.A. All authors have read and agreed to the published version of the manuscript.

Funding: This research received no external funding.

Institutional Review Board Statement: Not applicable.

Informed Consent Statement: Not applicable.

Data Availability Statement: All genomes are available in the NCBI database.

Acknowledgments: We would like to thank the agencies Coordination for the Improvement of Higher Education Personnel (CAPES), Minas Gerais Research Funding Foundation (FAPEMIG) for the Post-Graduate Support Program (PAPG) scholarship ID-11713 5.18/2022, and Pernambuco Research Funding Foundation (FACEPE) for Institutional Scientific Initiation Scholarship Program (PIBIC) BIC-2027-22/17. We would also like to thank the Post Graduate Program in Bioinformatics at the Federal University of Minas Gerais.

Conflicts of Interest: The authors declare no conflict of interest.

Appendix A. General Information Regarding Genomes Used in This Work

All information was retrieved from NCBI, both for *Xanthomonas campestris* and *Xanthomonas citri*.

Table A1. Relevant information for the *X. campestris* and *X. citri* strains.

Species [18]	Strains	BioProject	Replicons	Assembly	Phytophacteriosis
<i>Xanthomonas arboricola</i> (Vauterin et al. 1995)	17	PRJNA280784	CP011256.1	GCA_000972745.1	Black rot of crucifers
<i>Xanthomonas campestris</i> pv. <i>campestris</i> (Pammel) Dowson	3811	PRJNA428847	NZ_CP025750.1	GCA_002879955.1	Black rot of crucifers
	B100	PRJNA29801	NC_010688.1	GCA_000070605.1	
	ICMP 21080	PRJNA283327	NZ_CP012145.1	GCA_001186415.1	
	ICMP 4013	PRJNA283326	NZ_CP012146.1	GCA_001186465.1	
	8004	PRJNA15	NC_007086.1	GCA_000012105.1	
	CN03	PRJNA211759	NZ_CP017308.1	GCA_002776735.1	
	CN18	PRJNA343742	NZ_CP017319.1	GCA_002776835.1	
	ATCC 33913	PRJNA296	NC_003902	GCA_000007145.1	
	CN12	PRJEB4853	NZ_CP017310.1	GCA_002776775.1	
	CN17	PRJNA211780	CP017307.1	GCA_002776715.1	
<i>Xanthomonas campestris</i> pv. <i>raphani</i> (White) Dye	756C	PRJNA63187	NC_017271.1	GCA_000221965.1	Black rot of crucifers
<i>Xanthomonas citri</i> pv. <i>anacardii</i> (Ah-You et al. 2009) [62]	IBSBF2579	PRJNA224116	NZ_PESI01000001.1	GCA_002837255.1	Bacterial black spot
	TAQ13	PRJNA224116	NZ_PESH01000000	GCA_002898475.1	
	TAQ18	PRJNA224116	NZ_PESG01000001.1	GCA_002898415.1	
<i>Xanthomonas citri</i> pv. <i>aurantifolii</i> (Ah-You et al. 2009)	1566	PRJNA273983	NZ_CP012002.1	GCA_001610915.1	Citrus canker
	FDC 1559	PRJNA273983	NZ_CP011160.1	GCA_001610795.1	
	FDC 1561	PRJNA273983	NZ_CP011250.1	GCA_002079965.1	
	FDC 1609	PRJNA273983	NZ_CP011163.1	GCA_001610815.1	
<i>Xanthomonas citri</i> pv. <i>fuscans</i> (Schaad et al. 2007)	ISO12C3	PRJNA289080	NZ_CP012055.1	GCA_003999505.1	Bacterial blight of bean
	ISO18C1	PRJNA289080	NZ_CP012053.1	GCA_003999485.1	
	ISO18C5	PRJNA289080	NZ_CP012051.1	GCA_004000475.1	
	4834-R	PRJNA176873	NC_022539.1	GCA_000969685.1	
<i>Xanthomonas citri</i> pv. <i>glycines</i> (Nakano, 2019)	12-2	PRJNA323439	NZ_CP015972.1	GCA_002163775.1	Bacterial pustule of soybean
	8ra	PRJNA341902	NZ_CP017188.1	GCA_001854145.2	
<i>Xanthomonas citri</i> pv. <i>phaseoli</i> var. <i>fuscans</i> (ex Smith, 1987) Dye 1978	CFBP4885	PRJNA384182	NZ_CP020992.1	GCA_002759355.2	Bacterial blight of bean
	CFBP6165	PRJNA384145	NZ_CP020998.1	GCA_002759215.3	
	CFBP6166	PRJNA384183	NZ_CP021001.1	GCA_002759235.2	
	CFBP6167	PRJNA384187	NZ_CP021018.1	GCA_002759415.2	
	CFBP6975	PRJNA384188	NZ_CP021006.1	GCA_002759255.3	
	CFBP6988R	PRJNA384160	NZ_CP020979.1	GCA_002759275.2	
	CFBP6989	PRJNA384161	NZ_CP020981.1	GCA_002759295.2	
	CFBP6990	PRJNA384163	NZ_CP020983.1	GCA_002759315.2	
	CFBP6991	PRJNA384178	NZ_CP021015.1	GCA_002759395.2	
	CFBP6992	PRJNA384177	NZ_CP020985.1	GCA_002759335.2	
	CFBP6994R	PRJNA384179	NZ_CP020987.1	GCA_002759175.2	

Table A1. Cont.

Species [18]	Strains	BioProject	Replicons	Assembly	Phytophacteriosis
<i>Xanthomonas citri</i> pv. <i>vignicola</i> (Burkholder, 1994)	CFBP6996R	PRJNA384180	NZ_CP020989.1	GCA_002759195.2	Bacterial blight of cowpea
	CFBP7767	PRJNA383319	NZ_CP021012.1	GCA_002759375.2	
	CFBP7111	PRJNA390891	NZ_CP022263.1	GCA_002218245.1	
	CFBP7112	PRJNA390892	NZ_CP022267.1	GCA_002218265.1	
	CFBP7113	PRJNA390890	NZ_CP022270.1	GCA_002218285.1	
<i>Xanthomonas citri</i> subsp. <i>citri</i> (Gabriel et al. 1989) Schaad et al. 2007	03-1638-1-1	PRJNA401937	NZ_CP023285.1	GCA_002952295.1	Citrus canker
	Xcc29-1	PRJNA407058	NZ_CP023661.1	GCA_003665475.1	
	Xcc49	PRJNA407058	NZ_CP023662.1	GCA_003665455.1	
	MSCT	PRJNA299817	NZ_CP017020.1	GCA_001719145.1	
	5208	PRJNA255042	NZ_CP009026.1	GCA_000961415.1	
	AW13	PRJNA255042	NZ_CP009029.1	GCA_000961435.1	
	AW14	PRJNA255042	NZ_CP009032.1	GCA_000961455.1	
	AW15	PRJNA255042	NZ_CP009035.1	GCA_000961475.1	
	AW16	PRJNA255042	NZ_CP009038.1	GCA_000961495.1	
	BL18	PRJNA255042	NZ_CP009023.1	GCA_000961395.1	
	FB19	PRJNA255042	NZ_CP009020.1	GCA_000961375.1	
	gd2	PRJNA255042	NZ_CP009017.1	GCA_000961355.1	
	gd3	PRJNA255042	NZ_CP009014.1	GCA_000961335.1	
	jx-6	PRJNA286060	NZ_CP011827.1	GCA_001028285.3	
	jx4	PRJNA255042	NZ_CP009011.1	GCA_000961315.1	
	jx5	PRJNA255042	NZ_CP009008.1	GCA_000961295.1	
	LH201	PRJNA344031	NZ_CP018858.1	GCA_001922105.1	
	LH276	PRJNA344031	NZ_CP018854.1	GCA_001922065.1	
	LJ207-7	PRJNA344031	NZ_CP018850.1	GCA_001922085.1	
	LL074-4	PRJNA344031	NZ_CP018847.1	GCA_001922045.1	
	mf20	PRJNA255042	NZ_CP009005.1	GCA_000961275.1	
	MN10	PRJNA255042	NZ_CP009002.1	GCA_000961255.1	
	MN11	PRJNA255042	NZ_CP008999.1	GCA_000961235.1	
	MN12	PRJNA255042	NZ_CP008996.1	GCA_000961215.1	
	NT17	PRJNA255042	NZ_CP008993.1	GCA_000961195.1	
	TX160042	PRJNA381640	NZ_CP020882.1	GCA_002139975.1	
	TX160149	PRJNA381640	NZ_CP020885.1	GCA_002139955.1	
	TX160197	PRJNA381640	NZ_CP020889.1	GCA_002139995.1	
	UI7	PRJNA255042	NZ_CP008987.1	GCA_000961155.1	
	306	PRJNA297	NC_003919.1	GCA_000007165.1	
	UI6	PRJNA255042	NZ_CP008990.1	GCA_000961175.1	

Table A1. Cont.

Species [18]	Strains	BioProject	Replicons	Assembly	Phytobacteriosis
<i>Xanthomonas citri</i> subsp. <i>malvacearum</i> (ex Smith 1901) Schaad et al. 2007	A306	PRJNA193618	NZ_CP006855.1	GCA_000816885.1	Bacterial blight of cotton
	Aw12879	PRJNA81931	NC_020815.	GCA_000349225.1	
	MS14003	PRJNA396899	NZ_CP023159.1	GCA_002288585.1	
	AR81009	PRJNA396899	NZ_CP023155.1	GCA_002288565.1	
	XcmH1005	PRJNA298765	NZ_CP013004.1	GCA_002224525.1	
<i>Xanthomonas vasicola</i> pv. <i>arecae</i> (Rao & Mohan) Dye 1978	XcmN1003	PRJNA298770	NZ_CP013006.1	GCA_002224545.1	Bacterial leaf streak of maize Xanthomonas wilt of banana
<i>Xanthomonas vasicola</i> pv. <i>musacearum</i> (Yirgou & Bradbury) Dye 1978	NCPPB 2649	PRJNA264725	CP034653.1	GCA_000770355.2	
	NCPPB 4379	PRJNA73877	NZ_CP034655.1	GCA_000277895.2	

Appendix B. Mobile Elements Found within *Xanthomonas* Genomes

Table A2. Number of Pathogenicity Islands (PAIs) found for each genome.

Species [18]	Strains	Number of PAIs
<i>Xanthomonas arboricola</i>	17	3
<i>Xanthomonas campestris</i> pv. <i>campestris</i>	8004	10
	CN03	6
	CN12	8
	CN17	7
	CN18	7
	3811	9
	ATCC 33913	10
	B100	7
	ICMP 21080	8
	ICMP 4013	7
<i>Xanthomonas campestris</i> pv. <i>raphani</i>	756C	4
<i>Xanthomonas citri</i> pv. <i>anacardii</i>	IBSBF2579	8
	TAQ13	7
	TAQ18	7
<i>Xanthomonas citri</i> pv. <i>aurantifolii</i>	1566	7
	FDC1559	11
	FDC1561	6
	FDC1609	8
<i>Xanthomonas citri</i> pv. <i>fuscans</i>	ISO118C1	4
	ISO118C5	3
	ISO12C3	3
	4834-R	4
<i>Xanthomonas citri</i> pv. <i>glycines</i>	12-2	7
	8ra	6
<i>Xanthomonas citri</i> pv. <i>phaseoli</i> var. <i>fuscans</i>	CFBP4885	7
	CFBP6165	4
	CFBP6166	4
	CFBP6167	3
	CFBP6975	4
	CFBP6988R	3
	CFBP6989	4
	CFBP6990	4
	CFBP6991	3
	CFBP6992	3
	CFBP6994R	5
	CFBP6996R	4
	CFBP7767	7
<i>Xanthomonas citri</i> pv. <i>vignicola</i>	CFBP7111	10
	CFBP7112	8
	CFBP7113	7
<i>Xanthomonas citri</i> subsp. <i>citri</i> (Gabriel et al. 1989) Schaad et al. 2007	306	8
	03-1638-1-1	9
	5208	8
	A306	9
	Aw12879	12
	AW13	13
	AW14	14
	AW15	11
	AW16	13
	BL18	9
	FB19	9
	gd2	7
	gd3	7
	jx-6	9

Table A2. Cont.

Species [18]	Strains	Number of PAIs
<i>Xanthomonas citri</i> subsp. <i>malvacearum</i> (ex Smith 1901) Schaad et al. 2007	jx4	8
	jx5	9
	LH201	9
	LH276	9
	LJ207-7	8
	LL074-4	8
	mf20	9
	MN10	9
	MN11	9
	MN12	9
	NT17	8
	TX160042	13
	TX160149	10
	TX160197	14
	UI6	7
	UI7	7
	Xcc29-1	9
	Xcc49	8
	AR81009	15
	MS14003	4
	MSCT	5
<i>Xanthomonas vasicola</i> pv. <i>arecae</i> <i>Xanthomonas vasicola</i> pv. <i>musacearum</i>	XcmH1005	13
	XcmN1003	10
	NCPPB2649	8
	NCPPB 4379	6

Table A3. Number of prophages regions in *Xanthomonas* genomes.

Strains	Intact Region	Questionable Region	Incomplete Region	Total Prophage Regions
<i>Xanthomonas arboricola</i> 17	4	0	0	4
<i>Xanthomonas campestris</i> pv. <i>campestris</i> CN17	1	1	0	2
<i>Xanthomonas campestris</i> pv. <i>campestris</i> 3811	0	1	0	1
<i>Xanthomonas campestris</i> pv. <i>campestris</i> 8004	2	0	0	2
<i>Xanthomonas campestris</i> pv. <i>campestris</i> ATCC 33913	2	1	0	3
<i>Xanthomonas campestris</i> pv. <i>campestris</i> B100	1	0	0	1
<i>Xanthomonas campestris</i> pv. <i>campestris</i> CN03	1	2	0	3
<i>Xanthomonas campestris</i> pv. <i>campestris</i> CN12	0	3	0	3
<i>Xanthomonas campestris</i> pv. <i>campestris</i> CN18	0	0	0	0
<i>Xanthomonas campestris</i> pv. <i>campestris</i> ICMP 21080	2	1	0	3
<i>Xanthomonas campestris</i> pv. <i>campestris</i> ICMP 4013	0	1	0	1
<i>Xanthomonas campestris</i> pv. <i>raphani</i> 756C	0	1	0	1
<i>Xanthomonas citri</i> pv. <i>anacardii</i> IBSBF2579	1	0	1	2
<i>Xanthomonas citri</i> pv. <i>anacardii</i> TAQ13	1	0	1	2
<i>Xanthomonas citri</i> pv. <i>anacardii</i> TAQ18	1	0	1	2
<i>Xanthomonas citri</i> pv. <i>aurantifolii</i> 1566	2	3	3	8
<i>Xanthomonas citri</i> pv. <i>aurantifolii</i> FDC1559	2	2	3	7
<i>Xanthomonas citri</i> pv. <i>aurantifolii</i> FDC1561	1	1	0	2
<i>Xanthomonas citri</i> pv. <i>aurantifolii</i> FDC1609	3	2	7	12
<i>Xanthomonas citri</i> pv. <i>fuscans</i> 4834-R	1	0	0	1
<i>Xanthomonas citri</i> pv. <i>fuscans</i> ISO118C1	1	0	0	1
<i>Xanthomonas citri</i> pv. <i>fuscans</i> ISO118C5	1	0	0	1
<i>Xanthomonas citri</i> pv. <i>fuscans</i> ISO12C3	1	0	0	1
<i>Xanthomonas citri</i> pv. <i>glycines</i> 12-2	3	1	1	5
<i>Xanthomonas citri</i> pv. <i>glycines</i> 8ra	4	1	0	5
<i>Xanthomonas citri</i> pv. <i>phaseoli</i> var. <i>fuscans</i> CFBP4885	1	0	0	1
<i>Xanthomonas citri</i> pv. <i>phaseoli</i> var. <i>fuscans</i> CFBP6165	1	0	0	1
<i>Xanthomonas citri</i> pv. <i>phaseoli</i> var. <i>fuscans</i> CFBP6166	1	0	0	1
<i>Xanthomonas citri</i> pv. <i>phaseoli</i> var. <i>fuscans</i> CFBP6167	1	0	0	1
<i>Xanthomonas citri</i> pv. <i>phaseoli</i> var. <i>fuscans</i> CFBP6975	2	0	0	2
<i>Xanthomonas citri</i> pv. <i>phaseoli</i> var. <i>fuscans</i> CFBP6988R	2	0	1	3
<i>Xanthomonas citri</i> pv. <i>phaseoli</i> var. <i>fuscans</i> CFBP6989	2	0	1	3
<i>Xanthomonas citri</i> pv. <i>phaseoli</i> var. <i>fuscans</i> CFBP6990	2	0	1	3

Table A3. Cont.

Strains	Intact Region	Questionable Region	Incomplete Region	Total Prophage Regions
<i>Xanthomonas citri</i> pv. <i>phaseoli</i> var. <i>fuscans</i> CFBP6991	2	0	1	3
<i>Xanthomonas citri</i> pv. <i>phaseoli</i> var. <i>fuscans</i> CFBP6992	1	0	0	1
<i>Xanthomonas citri</i> pv. <i>phaseoli</i> var. <i>fuscans</i> CFBP6994R	2	0	0	2
<i>Xanthomonas citri</i> pv. <i>phaseoli</i> var. <i>fuscans</i> CFBP6996R	1	0	0	1
<i>Xanthomonas citri</i> pv. <i>phaseoli</i> var. <i>fuscans</i> CFBP7767	1	0	0	1
<i>Xanthomonas citri</i> pv. <i>vignicola</i> CFBP7111	4	0	4	8
<i>Xanthomonas citri</i> pv. <i>vignicola</i> CFBP7112	1	1	0	2
<i>Xanthomonas citri</i> pv. <i>vignicola</i> CFBP7113	2	1	3	6
<i>Xanthomonas citri</i> subsp. <i>citri</i> 03-1638-1-1	1	2	1	4
<i>Xanthomonas citri</i> subsp. <i>citri</i> 5208	1	1	2	4
<i>Xanthomonas citri</i> subsp. <i>citri</i> A306	1	1	2	4
<i>Xanthomonas citri</i> subsp. <i>citri</i> Aw12879	3	1	2	6
<i>Xanthomonas citri</i> subsp. <i>citri</i> AW13	3	1	2	6
<i>Xanthomonas citri</i> subsp. <i>citri</i> AW14	3	1	2	6
<i>Xanthomonas citri</i> subsp. <i>citri</i> AW15	3	1	2	6
<i>Xanthomonas citri</i> subsp. <i>citri</i> AW16	3	1	2	6
<i>Xanthomonas citri</i> subsp. <i>citri</i> BL18	1	1	2	4
<i>Xanthomonas citri</i> subsp. <i>citri</i> FB19	1	1	2	4
<i>Xanthomonas citri</i> subsp. <i>citri</i> gd2	1	1	2	4
<i>Xanthomonas citri</i> subsp. <i>citri</i> gd3	1	1	2	4
<i>Xanthomonas citri</i> subsp. <i>citri</i> jx-6	1	1	1	3
<i>Xanthomonas citri</i> subsp. <i>citri</i> jx4	1	1	2	4
<i>Xanthomonas citri</i> subsp. <i>citri</i> jx5	1	1	2	4
<i>Xanthomonas citri</i> subsp. <i>citri</i> LH201	1	1	1	3
<i>Xanthomonas citri</i> subsp. <i>citri</i> LH276	1	2	1	4
<i>Xanthomonas citri</i> subsp. <i>citri</i> LJ207-7	1	2	1	4
<i>Xanthomonas citri</i> subsp. <i>citri</i> LL074-4	1	2	1	4
<i>Xanthomonas citri</i> subsp. <i>citri</i> mf20	1	1	2	4
<i>Xanthomonas citri</i> subsp. <i>citri</i> MN10	1	1	2	4
<i>Xanthomonas citri</i> subsp. <i>citri</i> MN11	1	1	2	4
<i>Xanthomonas citri</i> subsp. <i>citri</i> MN12	1	1	2	4
<i>Xanthomonas citri</i> subsp. <i>citri</i> NT17	1	1	2	4
<i>Xanthomonas citri</i> subsp. <i>citri</i> str. 306	0	0	0	0

Table A3. Cont.

Strains	Intact Region	Questionable Region	Incomplete Region	Total Prophage Regions
<i>Xanthomonas citri</i> subsp. <i>citri</i> TX160042	3	1	0	4
<i>Xanthomonas citri</i> subsp. <i>citri</i> TX160149	2	1	3	6
<i>Xanthomonas citri</i> subsp. <i>citri</i> TX160197	3	1	0	4
<i>Xanthomonas citri</i> subsp. <i>citri</i> UI6	1	1	2	4
<i>Xanthomonas citri</i> subsp. <i>citri</i> UI7	1	1	2	4
<i>Xanthomonas citri</i> subsp. <i>citri</i> Xcc29-1	1	1	1	3
<i>Xanthomonas citri</i> subsp. <i>citri</i> Xcc49	1	1	1	3
<i>Xanthomonas citri</i> subsp. <i>malvacearum</i> AR81009	0	0	0	0
<i>Xanthomonas citri</i> subsp. <i>malvacearum</i> MS14003	2	0	1	3
<i>Xanthomonas citri</i> subsp. <i>malvacearum</i> MSCT	1	0	0	1
<i>Xanthomonas citri</i> subsp. <i>malvacearum</i> XcmH1005	0	2	0	2
<i>Xanthomonas citri</i> subsp. <i>malvacearum</i> XcmN1003	3	1	1	5
<i>Xanthomonas vasicola</i> pv. <i>arecae</i> NCPPB2649	1	2	0	3
<i>Xanthomonas vasicola</i> pv. <i>musacearum</i> NCPPB 4379	2	0	1	3

References

1. Chagas, M.C.M.; Parra, J.R.P.; Namekata, T.; Hartung, J.S.; Yamamoto, P.T. *Phyllocnistis citrella* Stainton (Lepidoptera: Gracillariidae) and its relationship with the citrus canker bacterium *Xanthomonas axonopodis* pv. *citri* in Brazil. *Neotrop. Entomol.* **2001**, *30*, 55–59. [\[CrossRef\]](#)
2. Nascimento, A.R.P.; Mariano, R.d.L.R. Cancro bacteriano da videira: Etiologia, epidemiologia e medidas de controle. *Cienc. Rural* **2004**, *34*, 301–307. [\[CrossRef\]](#)
3. Iglesias-Bernabé, L.; Madloo, P.; Rodríguez, V.M.; Francisco, M.; Soengas, P. Dissecting quantitative resistance to *Xanthomonas campestris* pv. *campestris* in leaves of *Brassica oleracea* by QTL analysis. *Sci. Rep.* **2019**, *9*, 2015. [\[CrossRef\]](#) [\[PubMed\]](#)
4. Batista, J.N.G.; Ferreira, M.A.d.S.V.; Quezado-Duval, A.M. Molecular and phenotypic characterization of *Xanthomonas campestris* pv. *campestris* causing black rot in *Brassica* crops in Brazil. *Trop. Plant Pathol.* **2021**, *46*, 684–701. [\[CrossRef\]](#)
5. Nuñez, A.M.P.; Rodríguez, G.A.A.; Monteiro, F.P.; Faria, A.F.; Silva, J.C.P.; Monteiro, A.C.A.; Carvalho, C.V.; Gomes, L.A.A.; Souza, R.M.; de Souza, J.T.; et al. Bio-based products control black rot (*Xanthomonas campestris* pv. *campestris*) and increase the nutraceutical and antioxidant components in kale. *Sci. Rep.* **2018**, *8*, 10199. [\[CrossRef\]](#) [\[PubMed\]](#)
6. Behlau, F. An overview of citrus canker in Brazil. *Trop. Plant Pathol.* **2021**, *46*, 1–12. [\[CrossRef\]](#)
7. Ference, C.M.; Gochez, A.M.; Behlau, F.; Wang, N.; Graham, J.H.; Jones, J.B. Recent advances in the understanding of *Xanthomonas citri* ssp. *citri* pathogenesis and citrus canker disease management. *Mol. Plant Pathol.* **2018**, *19*, 1302–1318. [\[CrossRef\]](#) [\[PubMed\]](#)
8. Lu, H.; Patil, P.; Van Sluys, M.A.; White, F.F.; Ryan, R.P.; Dow, J.M.; Rabinowicz, P.; Salzberg, S.L.; Leach, J.E.; Sonti, R.; et al. Acquisition and Evolution of Plant Pathogenesis-Associated Gene Clusters and Candidate Determinants of Tissue-Specificity in *Xanthomonas*. *PLoS ONE* **2008**, *3*, e3828. [\[CrossRef\]](#) [\[PubMed\]](#)
9. Hersemann, L.; Wibberg, D.; Blom, J.; Goesmann, A.; Widmer, F.; Vorhölter, F.J.; Kölliker, R. Comparative genomics of host adaptive traits in *Xanthomonas translucens* pv. *graminis*. *BMC Genom.* **2017**, *18*, 35. [\[CrossRef\]](#) [\[PubMed\]](#)
10. Jacques, M.A.; Arlat, M.; Boulanger, A.; Boureau, T.; Carrère, S.; Cesbron, S.; Chen, N.W.; Cociancich, S.; Darrasse, A.; Denancé, N.; et al. Using Ecology, Physiology, and Genomics to Understand Host Specificity in *Xanthomonas*. *Annu. Rev. Phytopathol.* **2016**, *54*, 163–187. [\[CrossRef\]](#) [\[PubMed\]](#)
11. Assis, R.A.B.; Varani, A.M.; Sagawa, C.H.D.; Patané, J.S.L.; Setubal, J.C.; Uceda-Campos, G.; da Silva, A.M.; Zaini, P.A.; Almeida, N.F.; Moreira, L.M.; et al. A comparative genomic analysis of *Xanthomonas arboricola* pv. *juglandis* strains reveal hallmarks of mobile genetic elements in the adaptation and accelerated evolution of virulence. *Genomics* **2021**, *113*, 2513–2525. [\[CrossRef\]](#) [\[PubMed\]](#)
12. Huang, C.J.; Wu, T.L.; Zheng, P.X.; Ou, J.Y.; Ni, H.F.; Lin, Y.C. Comparative Genomic Analysis Uncovered Evolution of Pathogenicity Factors, Horizontal Gene Transfer Events, and Heavy Metal Resistance Traits in Citrus Canker Bacterium *Xanthomonas citri* subsp. *citri*. *Front. Microbiol.* **2021**, *12*, 731711. [\[CrossRef\]](#) [\[PubMed\]](#)
13. Loper, J.E.; Hassan, K.A.; Mavrodi, D.V.; Davis, E.W.; Lim, C.K.; Shaffer, B.T.; Elbourne, L.D.H.; Stockwell, V.O.; Hartney, S.L.; Breakwell, K.; et al. Comparative Genomics of Plant-Associated *Pseudomonas* spp.: Insights into Diversity and Inheritance of Traits Involved in Multitrophic Interactions. *PLoS Genet.* **2012**, *8*, e1002784. [\[CrossRef\]](#)
14. Hajri, A.; Brin, C.; Hunault, G.; Lardeux, F.; Lemaire, C.; Manceau, C.; Boureau, T.; Poussier, S. A «repertoire for repertoire» hypothesis: Repertoires of type three effectors are candidate determinants of host specificity in *Xanthomonas*. *PLoS ONE* **2009**, *4*, e6632. [\[CrossRef\]](#)
15. Kay, S.; Bonas, U. How *Xanthomonas* type III effectors manipulate the host plant. *Curr. Opin. Microbiol.* **2009**, *12*, 37–43. [\[CrossRef\]](#) [\[PubMed\]](#)
16. Timilsina, S.; Pereira-Martin, J.A.; Minsavage, G.V.; Iruegas-Bocardo, F.; Abrahamian, P.; Potnis, N.; Kolaczowski, B.; Vallad, G.E.; Goss, E.M.; Jones, J.B. Multiple Recombination Events Drive the Current Genetic Structure of *Xanthomonas perforans* in Florida. *Front. Microbiol.* **2019**, *10*, 448. [\[CrossRef\]](#) [\[PubMed\]](#)
17. da Gama, M.A.S.; Mariano, R.d.L.R.; da Silva Júnior, W.J.; de Farias, A.R.G.; Barbosa, M.A.G.; Ferreira, M.Á.d.S.V.; Costa Júnior, C.R.L.; Santos, L.A.; de Souza, E.B. Taxonomic Repositioning of *Xanthomonas campestris* pv. *viticola* (Nayudu 1972) Dye 1978 as *Xanthomonas citri* pv. *viticola* (Nayudu 1972) Dye 1978 comb. nov. and Emendation of the Description of *Xanthomonas citri* pv. *anacardii* to Include Pigmented Isolates Pathogenic to Cashew Plant. *Phytopathology* **2018**, *108*, 1143–1153. [\[CrossRef\]](#) [\[PubMed\]](#)
18. Constantin, E.C.; Cleenwerck, I.; Maes, M.; Baeyen, S.; Van Malderghem, C.; De Vos, P.; Cottyn, B. Genetic characterization of strains named as *Xanthomonas axonopodis* pv. *dieffenbachiae* leads to a taxonomic revision of the *X. axonopodis* species complex. *Plant Pathol.* **2016**, *65*, 792–806. [\[CrossRef\]](#)
19. Cesbron, S.; Briand, M.; Essakhi, S.; Gironde, S.; Boureau, T.; Manceau, C.; Fischer-Le Saux, M.; Jacques, M.A. Comparative Genomics of Pathogenic and Nonpathogenic Strains of *Xanthomonas arboricola* Unveil Molecular and Evolutionary Events Linked to Pathoadaptation. *Front. Plant Sci.* **2015**, *6*, 1126. [\[CrossRef\]](#) [\[PubMed\]](#)
20. Studholme, D.J.; Wicker, E.; Abrare, S.M.; Aspin, A.; Bogdanove, A.; Broders, K.; Dubrow, Z.; Grant, M.; Jones, J.B.; Karamura, G.; et al. Transfer of *Xanthomonas campestris* pv. *arecae* and *X. campestris* pv. *musacearum* to *X. vasicola* (Vauterin) as *X. vasicola* pv. *arecae* comb. nov. and *X. vasicola* pv. *musacearum* comb. nov. and Description of *X. vasicola* pv. *vasculorum* pv. nov. *Phytopathology* **2020**, *110*, 1153–1160. [\[CrossRef\]](#)
21. Aziz, R.K.; Bartels, D.; Best, A.A.; DeJongh, M.; Disz, T.; Edwards, R.A.; Formsma, K.; Gerdes, S.; Glass, E.M.; Kubal, M.; et al. The RAST Server: Rapid Annotations using Subsystems Technology. *BMC Genom.* **2008**, *9*, 75. [\[CrossRef\]](#) [\[PubMed\]](#)

22. Carver, T.; Berriman, M.; Tivey, A.; Patel, C.; Böhme, U.; Barrell, B.G.; Parkhill, J.; Rajandream, M.A. Artemis and ACT: Viewing, annotating and comparing sequences stored in a relational database. *Bioinformatics* **2008**, *24*, 2672–2676. [\[CrossRef\]](#) [\[PubMed\]](#)
23. Araujo, F.A.; Barh, D.; Silva, A.; Guimarães, L.; Ramos, R.T.J. GO FEAT: A rapid web-based functional annotation tool for genomic and transcriptomic data. *Sci. Rep.* **2018**, *8*, 1794. [\[CrossRef\]](#)
24. Kanehisa, M. The KEGG resource for deciphering the genome. *Nucleic Acids Res.* **2004**, *32*, 277D–D280. [\[CrossRef\]](#)
25. Chaudhari, N.M.; Gupta, V.K.; Dutta, C. BPGA—An ultra-fast pan-genome analysis pipeline. *Sci. Rep.* **2016**, *6*, 24373. [\[CrossRef\]](#)
26. Page, A.J.; Cummins, C.A.; Hunt, M.; Wong, V.K.; Reuter, S.; Holden, M.T.; Fookes, M.; Falush, D.; Keane, J.A.; Parkhill, J. Roary: Rapid large-scale prokaryote pan genome analysis. *Bioinformatics* **2015**, *31*, 3691–3693. [\[CrossRef\]](#) [\[PubMed\]](#)
27. Rambaut, A. FigTree—Version 1.4. 3, a Graphical Viewer of Phylogenetic Trees. 2017. Computer program distributed by the author. Available online: <http://tree.bio.ed.ac.uk/software/figtree> (accessed on 10 September 2022).
28. Chen, L.; Yang, J.; Yu, J.; Yao, Z.; Sun, L.; Shen, Y.; Jin, Q. VFDB: A reference database for bacterial virulence factors. *Nucleic Acids Res.* **2005**, *33*, D325–D328. [\[CrossRef\]](#) [\[PubMed\]](#)
29. Soares, S.C.; Geyik, H.; Ramos, R.T.J.; de Sá, P.H.C.G.; Barbosa, E.G.V.; Baumbach, J.; Figueiredo, H.C.P.; Miyoshi, A.; Tauch, A.; Silva, A.; et al. GIPSY: Genomic island prediction software. *J. Biotechnol.* **2016**, *232*, 2–11. [\[CrossRef\]](#) [\[PubMed\]](#)
30. Bertelli, C.; Brinkman, F.S.L. Improved genomic island predictions with IslandPath-DIMOB. *Bioinformatics* **2018**, *34*, 2161–2167. [\[CrossRef\]](#) [\[PubMed\]](#)
31. Alikhan, N.F.; Petty, N.K.; Ben Zakour, N.L.; Beatson, S.A. BLAST Ring Image Generator (BRIG): Simple prokaryote genome comparisons. *BMC Genom.* **2011**, *12*, 402. [\[CrossRef\]](#)
32. Darling, A.C.E.; Mau, B.; Blattner, F.R.; Perna, N.T. Mauve: Multiple alignment of conserved genomic sequence with rearrangements. *Genome Res.* **2004**, *14*, 1394–1403. [\[CrossRef\]](#) [\[PubMed\]](#)
33. Yu, N.Y.; Wagner, J.R.; Laird, M.R.; Melli, G.; Rey, S.; Lo, R.; Dao, P.; Sahinalp, S.C.; Ester, M.; Foster, L.J.; et al. PSORTb 3.0: Improved protein subcellular localization prediction with refined localization subcategories and predictive capabilities for all prokaryotes. *Bioinformatics* **2010**, *26*, 1608–1615. [\[CrossRef\]](#) [\[PubMed\]](#)
34. Arndt, D.; Grant, J.R.; Marcu, A.; Sajed, T.; Pon, A.; Liang, Y.; Wishart, D.S. PHASTER: A better, faster version of the PHAST phage search tool. *Nucleic Acids Res.* **2016**, *44*, W16–W21. [\[CrossRef\]](#)
35. Singh, A.; Bansal, K.; Kumar, S.; Patil, P.B. Deep Population Genomics Reveals Systematic and Parallel Evolution at a Lipopolysaccharide Biosynthetic Locus in *Xanthomonas* Pathogens That Infect Rice and Sugarcane. *Appl. Environ. Microbiol.* **2022**, *88*, e00550–22. [\[CrossRef\]](#)
36. Zarei, S.; Taghavi, S.M.; Rahimi, T.; Mafakheri, H.; Potnis, N.; Koebnik, R.; Fischer-Le Saux, M.; Pothier, J.F.; Palacio Bielsa, A.; Cubero, J.; et al. Taxonomic Refinement of *Xanthomonas arboricola*. *Phytopathology* **2022**, *112*, 1630–1639. [\[CrossRef\]](#) [\[PubMed\]](#)
37. Rana, R.; Madhavan, V.N.; Saroha, T.; Bansal, K.; Kaur, A.; Sonti, R.V.; Patel, H.K.; Patil, P.B. *Xanthomonas indica* sp. nov., a Novel Member of Non-Pathogenic *Xanthomonas* Community from Healthy Rice Seeds. *Curr. Microbiol.* **2022**, *79*, 304. [\[CrossRef\]](#) [\[PubMed\]](#)
38. Cho, H.; Song, E.S.; Heu, S.; Baek, J.; Lee, Y.K.; Lee, S.; Lee, S.W.; Park, D.S.; Lee, T.H.; Kim, J.G.; et al. Prediction of Host-Specific Genes by Pan-Genome Analyses of the Korean *Ralstonia solanacearum* Species Complex. *Front. Microbiol.* **2019**, *10*, 506. [\[CrossRef\]](#)
39. Kang, I.J.; Kim, K.S.; Beattie, G.A.; Yang, J.W.; Sohn, K.H.; Heu, S.; Hwang, I. Pan-Genome Analysis of Effectors in Korean Strains of the Soybean Pathogen *Xanthomonas citri* pv. *glycines*. *Microorganisms* **2021**, *9*, 2065. [\[CrossRef\]](#)
40. Patil, P.P.; Midha, S.; Kumar, S.; Patil, P.B. Genome Sequence of Type Strains of Genus *Stenotrophomonas*. *Front. Microbiol.* **2016**, *7*, 309. [\[CrossRef\]](#)
41. Thieme, F.; Koebnik, R.; Bekel, T.; Berger, C.; Boch, J.; Büttner, D.; Caldana, C.; Gaigalat, L.; Goesmann, A.; Kay, S.; et al. Insights into Genome Plasticity and Pathogenicity of the Plant Pathogenic Bacterium *Xanthomonas campestris* pv. *vesicatoria* Revealed by the Complete Genome Sequence. *J. Bacteriol.* **2005**, *187*, 7254–7266. [\[CrossRef\]](#)
42. Souza, D.P.; Oka, G.U.; Alvarez-Martinez, C.E.; Bisson-Filho, A.W.; Dunger, G.; Hobeika, L.; Cavalcante, N.S.; Alegria, M.C.; Barbosa, L.R.; Salinas, R.K.; et al. Bacterial killing via a type IV secretion system. *Nat. Commun.* **2015**, *6*, 6453. [\[CrossRef\]](#) [\[PubMed\]](#)
43. Bansal, K.; Midha, S.; Kumar, S.; Patil, P.B. Ecological and Evolutionary Insights into *Xanthomonas citri* Pathovar Diversity. *Appl. Environ. Microbiol.* **2017**, *83*. [\[CrossRef\]](#) [\[PubMed\]](#)
44. Johnson, C.M.; Grossman, A.D. Integrative and Conjugative Elements (ICEs): What They Do and How They Work. *Annu. Rev. Genet.* **2015**, *49*, 577–601. [\[CrossRef\]](#) [\[PubMed\]](#)
45. Hallstrom, K.N.; McCormick, B.A. Pathogenicity Islands. In *Molecular Medical Microbiology*; Elsevier: Amsterdam, The Netherlands, 2015; pp. 303–314. [\[CrossRef\]](#)
46. Sgro, G.G.; Oka, G.U.; Souza, D.P.; Cenens, W.; Bayer-Santos, E.; Matsuyama, B.Y.; Bueno, N.F.; dos Santos, T.R.; Alvarez-Martinez, C.E.; Salinas, R.K.; et al. Bacteria-Killing Type IV Secretion Systems. *Front. Microbiol.* **2019**, *10*, 1078. [\[CrossRef\]](#) [\[PubMed\]](#)
47. Katzen, F.; Ferreira, D.U.; Oddo, C.G.; Ielmini, M.V.; Becker, A.; Pühler, A.; Ielpi, L. *Xanthomonas campestris* pv. *campestris* gum Mutants: Effects on Xanthan Biosynthesis and Plant Virulence. *J. Bacteriol.* **1998**, *180*, 1607–1617. [\[CrossRef\]](#) [\[PubMed\]](#)
48. Capage, M.; Doherty, D.H.; Betlach, M.; Vanderslice, R.W. Recombinant-DNA mediated production of xanthan gum. *Biotechnology Advances* **1997**, *15*, 547–547.

49. Büttner, D.; Noël, L.; Thieme, F.; Bonas, U. Genomic approaches in *Xanthomonas campestris* pv. *vesicatoria* allow fishing for virulence genes. *J. Biotechnol.* **2003**, *106*, 203–214. [\[CrossRef\]](#)
50. Han, S.W.; Hwang, B.K. Molecular functions of *Xanthomonas* type III effector AvrBsT and its plant interactors in cell death and defense signaling. *Planta* **2017**, *245*, 237–253. [\[CrossRef\]](#)
51. Dong, Q.; Ebricht, R.H. DNA binding specificity and sequence of *Xanthomonas campestris* catabolite gene activator protein-like protein. *J. Bacteriol.* **1992**, *174*, 5457–5461. [\[CrossRef\]](#)
52. de Crecy-Lagard, V.; Glaser, P.; Lejeune, P.; Sismeiro, O.; Barber, C.E.; Daniels, M.J.; Danchin, A. A *Xanthomonas campestris* pv. *campestris* protein similar to catabolite activation factor is involved in regulation of phytopathogenicity. *J. Bacteriol.* **1990**, *172*, 5877–5883. [\[CrossRef\]](#)
53. Payne, S.M. Iron acquisition in microbial pathogenesis. *Trends Microbiol.* **1993**, *1*, 66–69. [\[CrossRef\]](#)
54. Jordan, M.R.; Wang, J.; Capdevila, D.A.; Giedroc, D.P. Multi-metal nutrient restriction and crosstalk in metallostasis systems in microbial pathogens. *Curr. Opin. Microbiol.* **2020**, *55*, 17–25. [\[CrossRef\]](#) [\[PubMed\]](#)
55. Zhang, P.; Jiang, D.; Wang, Y.; Yao, X.; Luo, Y.; Yang, Z. Comparison of De Novo Assembly Strategies for Bacterial Genomes. *Int. J. Mol. Sci.* **2021**, *22*, 7668. [\[CrossRef\]](#) [\[PubMed\]](#)
56. Sharma, A.; Sharma, D.; Verma, S.K. In silico identification of copper-binding proteins of *Xanthomonas translucens* pv. *undulosa* for their probable role in plant-pathogen interactions. *PMPP Physiol. Mol. Plant Pathol.* **2019**, *106*, 187–195. [\[CrossRef\]](#)
57. Lima, W.C.; Paquola, A.C.; Varani, A.M.; Van Sluys, M.A.; Menck, C.F. Laterally transferred genomic islands in *Xanthomonadales* related to pathogenicity and primary metabolism: LGT islands in *Xanthomonas*. *FEMS Microbiol. Lett.* **2008**, *281*, 87–97. [\[CrossRef\]](#)
58. Cabrejos, D.A.L.; Alexandrino, A.V.; Pereira, C.M.; Mendonça, D.C.; Pereira, H.D.; Novo-Mansur, M.T.M.; Garratt, R.C.; Goto, L.S. Structural characterization of a pathogenicity-related superoxide dismutase codified by a probably essential gene in *Xanthomonas citri* subsp. *citri*. *PLoS ONE* **2019**, *14*, e0209988. [\[CrossRef\]](#)
59. O'Brien, J.A.; Daudi, A.; Butt, V.S.; Paul Bolwell, G. Reactive oxygen species and their role in plant defence and cell wall metabolism. *Planta* **2012**, *236*, 765–779. [\[CrossRef\]](#)
60. Canchaya, C.; Fournous, G.; Brüssow, H. The impact of prophages on bacterial chromosomes: Prophage-chromosome interaction. *Mol. Microbiol.* **2004**, *53*, 9–18. [\[CrossRef\]](#)
61. da Silva, A.C.R.; Ferro, J.A.; Reinach, F.C.; Farah, C.S.; Furlan, L.R.; Quaggio, R.B.; Monteiro-Vitorello, C.B.; Van Sluys, M.A.; Almeida, N.F.; Alves, L.M.C.; et al. Comparison of the genomes of two *Xanthomonas* pathogens with differing host specificities. *Nature* **2002**, *417*, 459–463. [\[CrossRef\]](#)
62. Silva Junior, W.J.; Farias, A.R.G.; Lima, N.B.; Benko-Iseppon, A.M.; Aburjaile, F.; Balbino, V.Q.; Falcão, R.M.; Leitão Paiva Júnior, S.d.S.; Sousa-Paula, L.C.; Mariano, R.L.R.; et al. Complete genome sequence of *Xanthomonas citri* pv. *anacardii* strain IBSBF2579 from Brazil. *Genome Announc.* **2018**, *6*, e01574-17. [\[CrossRef\]](#)